Supporting Information

Mease et al. 10.1073/pnas.1318665111

SI Discussion

Role of Membrane Potential Fluctuations in Thalamic Adaptation. In addition to depolarization, cortical layer 6 (L6) activation robustly increased membrane potential fluctuations in ventro-posteromedial nucleus (VPM) neurons (Fig. S8). It has been widely demonstrated that increases in background synaptic activity can strongly affect single-neuron spiking properties (1–8). Specific to the thalamus, the results we report here are complementary to the in vitro reports of Wolfart et al. (8), who showed that synaptic noise both blurred discrete burst/tonic thalamic firing modes and boosted the probability of response to small inputs by linearizing thalamic input/output curves. We show here that in vivo the L6-induced decrease in the contribution of low-threshold calcium spikes (LTS) to excitatory postsynaptic potentials (EPSPs) evoked by high-frequency sensory stimuli can be offset by the underlying depolarization itself, thereby decreasing adaptation (Fig. 5). However, it is possible that this effect is enhanced by the accompanying increase in membrane potential fluctuations by either graded recruitment of low-threshold calcium current (I_T) (8) via deinactivation and consequent heightening of I_T's role in excitability at depolarized membrane potentials (9) or a similar recruitment of sodium channels controlling action potential (AP) generation (6).

Role of the L6 Cortico–Thalamic Pathway. Previous studies of the L6 cortico–thalamic pathway do not create an entirely cohesive picture of its network functions. Recently, Olsen et al. (10) showed no effect of targeted L6 activation on the thalamic dorsal lateral geniculate nucleus response mode, whereas earlier studies showed either no effect after general inhibition of the visual cortical column (11) or a change of response modes in both directions after hyperactivation of L6 (12). In the visual thalamus, L6 activation reduced both responsiveness and burstiness; however, the latter effect was, in contrast to our study, not significant. These discrepancies among different studies suggest that, in addition to anatomical alignment, the direction of the mode shift is determined by the relative timing of L6 activity and sensory input. In this scheme, brief activation of L6 may guarantee burst firing via recruitment of the reticular nucleus (13), resulting in the cortex receiving a "wake-up call from the thalamus" (14, 15). In contrast, longer periods of L6 activity—for example, as a result of motion (16, 17)—may promote the tonic mode of operation through the direct L6 cortico–thalamic depolarization described here.

SI Methods

All experiments were done according to German animal welfare guidelines and were approved by the ethical committees of the Technical University of Munich.

Stereotaxic Injection. Stereotaxic injections of male and female Ntsr1 mice (founder line GN220) were done at postnatal day 30–40 using isofluorane anesthesia. After a small incision was made in the skin, the head was leveled with an electronic leveling device (Sigmann Elektronik). A craniotomy was made 3 mm lateral and 1 mm posterior to bregma. Then 250 nL of Adeno-associated viral (AAV) particles encoding for DIO-ChR2-mCherry (Genedetect), were distributed over four target sites in the BC with the following coordinates [in mm] relative to bregma, midline, and dura: −1, 2.9, −1; −1, 3.3, −1.1; −1.4, 2.9, −1; and −1.4, 3.3, −1.1. Mice then were sutured and housed in their cages until the experiment. Incubation time was 10–20 d.

Animal Preparation and Recordings. Animal preparation and recordings were done under Isofluorane anesthesia, 0.8–1.2% (vol/vol) in O_2 applied via a SurgiVet Vaporizer. Depth of anesthesia was monitored (Labchart) by keeping the respiratory rate constant at ∼130 beats per minute. A craniotomy was made above the VPM (2 mm lateral and 1.6 mm posterior from bregma), and the head was stereotaxically aligned for precise targeting of the VPM. All recordings were done in the right hemisphere at a depth of 3.2–3.5 mm from dura mater. VPM neurons were identified by their robust responses to whisker deflections, typically of one principal whisker by a hand-held probe. In vivo juxtacellular recordings and biocytin fillings were made with 4.5–5.5 MΩ patch pipettes pulled from borosilicate filamented glass (Hilgenber) on a DMZ Universal puller (Zeitz Instruments). Pipettes were filled with (in mM) 135 NaCl, 5.4 KCl, 1.8 CaCl2, 1 $MgCl_2$, and 5 Hepes, pH adjusted to 7.2 with NaOH, and 20 mg/mL biocytin was added. The bath solution was identical without biocytin. Single units were found by the 2× increase of pipette resistance measured in voltage-clamp mode. Single-unit recordings were made using an ELC-01X amplifier (NPI Electronics). Unfiltered and band-pass–filtered signals (high pass: 300 Hz, low pass: 9000 Hz) were digitized at 20 kHz with a CED Micro 1401 mkII board and were acquired using Spike2 software (both from Cambridge Electronic Design). Typically, recordings consisted of one single unit which was filled at the end of the experiment with biocytin using current pulses. Whole-cell voltage recordings in the VPM were done blindly with low-resistance patch pipettes (5-6.5 MΩ) as described in ref. 18. The pipette solution was (in mM) 130 K-gluconate, 10 Hepes, 10 Na-phosphocreatine, 10 Na-gluconate, 4 ATP-$Mg2^+$, 4 NaCl, 0.3 GTP, 0.1 EGTA, and 2 mg/mL biocytin. The osmolarity was ∼300 and was brought to pH 7.2 with KOH.

Whisker Stimulation. Whiskers were cut to a length of 1 cm. After the principle whisker was identified with a hand-held probe, the whisker tip was put into a short (2-mm) glass capillary (i.d. ∼100 μm) glued to a piezo wafer with high resonance frequency (380 Hz; PL127.1; Physics Instruments). Stimulation was controlled with an amplifier and a filter (Sigmann Elektronik). Pulses consisted of square 50-ms pulses for juxtacellular recordings and square 2-ms pulses for intracellular recordings. The rostral-to-caudal displacement of the whisker was 0.5–1 mm.

In Vivo Laser Stimulation of L6. A custom-built laser setup was used for optical fiber-based stimulation of ChR2-expressing L6 neurons. The stimulation light was delivered by a solid-state laser (Sapphire; Coherent) with a wavelength of 488 nm and a maximal output power of 50 mW. Pulses were controlled with an ultrafast shutter (Uniblitz). The laser beam was focused by means of a collimator into one end of a multimode fiber (Thorlabs) with a numerical aperture of 0.48 and an i.d. of 125 μm. The power density was 34–154 mW/mm^2, and 34 mW/mm^2 were used for the combined whisker and laser experiments. Shutter control was implemented with Spike2 software (Cambridge Electronic Design).

Histology. After the recordings the animal was given a lethal injection of ketamine/xylazine and was perfused transcardially with 4% paraformaldehyde in 0.1 M PBS. The brain was removed and postfixated for 4–8 h. Cell location and morphologies were revealed by tissue staining with streptavidin-Alexa-647 (Invitrogen) as described in ref. 19 Layer borders (Fig. 1*B* and Fig. S1) were estimated based on variations in soma density and soma size

after the somata were visualized with a fluorescent Nissl stain (Neurotrace; Invitrogen).

Data Analysis. Data were imported from Spike2 and analyzed using custom-written Matlab software (MathWorks) and JMP 3.2 (SAS Institute).

Spike times were extracted from the voltage trace by thresholding the temporal derivative typically at 50% of the maximum signal. Peristimulus time histograms (PSTHs) were calculated using 18–294 repetitions of whisker deflection and/or L6 photostimulation with a bin size of 2 ms.

A stimulus presentation was considered successful if one or more spikes were generated within 50 ms of stimulus onset or offset. The probability of response was calculated as the number of success trials divided by the number of total stimulus presentations. Stimulus (whisker or L6-evoked) activity was compared with spontaneous activity using a χ^2 test between spike counts in temporal intervals of comparable length.

Responses were sorted into single-spike (tonic) and burst response events using an ISI criterion. Any spike preceded by an ISI of less than 10 ms was considered part of a burst response event, e.g., four spikes with corresponding ISIs of 20, 4, 9, and 35 ms would be classified as two discrete events: a burst of three spikes followed by a tonic spike. We decided to use this 10-ms criterion, which is less stringent than the often-used 4-ms criterion (20), because calcium spike-mediated bursts in our intracellular data often had ISIs >4 ms (Fig. 3*B*). The conclusion that L6 input controls the size of the calcium spike and thereby shifts the thalamus toward tonic responses was independent of the exact ISI cutoff, because varying the ISI criterion between 5 and 20 ms changed event-sorting results only rarely and did not affect the trends on which we based our conclusions.

Burst probability was calculated as the number of successful trials in which a burst was elicited divided by the total number of successful trials. Mean spike count per response was calculated as the average number of spikes in the first response event elicited by a stimulus; successive events seldom occurred and were not analyzed further. Although the probability of a burst and the number of spikes per response metrics are redundant and naturally correlated, the number of spikes measure has the advantage of illustrating the graded effect of L6 input we observed, in that cortical feedback at times decreased the number of spikes per burst rather driving a full switch to tonic firing.

Adaptation Analysis. The probability of response was determined as the ratio of trials with a successful spike response (regardless of the number of spikes per response) to the trials without a spike response within 50 ms after the onset of each whisker stimulus in the train. The significance of the L6 effect on response probability was analyzed using a two-way within-subjects repeated-measures ANOVA in combination with a contrast analysis to determine significant differences between groups [The first stimulation, in a train of eight successive stimulations, of whisker only (W-1) compared with a stimulus train of the same whisker plus L6 activation (WL-1). The second stimulation W-2 compared with WL-2, and so forth.]. The probability of response to successive stimulations decreased [main effect of stimulation number: $F(7, 63) = 21.53$, $P < 0.0001$], but this effect was reduced when the whisker stimulation was combined with the activation of L6 corticothalamic neurons [interaction between stimulation number and treatment (whisker-only or whisker and L6 activation): $F(7, 63) = 2.66$, $P = 0.018$; main effect of treatment: $F(1, 9) = 1.47$, $P = 0.26$]. Thus, activation of L6 increased the probability of response (contrast analysis: W-1 vs. WL-1: $P = 0.08$; W-2 vs. WL-2: $P = 0.03$; W-3 vs. WL-3: $P = 0.005$; W-4 vs. WL-4: $P = 0.005$; W-5 vs. WL-5: $P = 0.008$; W-6 vs. WL-6: $P = 0.05$; W-7 vs. WL-7: $P = 0.012$; W-8 vs. WL-8: $P = 0.014$).

Membrane Fluctuation Analysis. Membrane potential SD (σ) was calculated using nine intracellular VPM recordings before and after L6 activation with no whisker stimulation (as in Fig. 1 and Fig. S4). As shown in Fig. S8, σ was calculated from 300-ms windows extracted before L6 onset (gray bar, control condition) and 200 ms after L6 activation (blue bar). To remove any slow depolarization changes associated with L6 activation or variation in membrane potential throughout the recording, each trace was detrended by subtracting the best linear fit to the voltage as a function of time; both APs (including $\pm$ 30 ms around each AP) and Ca LTS and following hyperpolarizations were excluded.

1. Chance FS, Abbott LF, Reyes AD (2002) Gain modulation from background synaptic input. *Neuron* 35(4):773–782.
2. McCormick DA, et al. (2003) Persistent cortical activity: Mechanisms of generation and effects on neuronal excitability. *Cereb Cortex* 13(11):1219–1231.
3. Shu Y, Hasenstaub A, Badoual M, Bal T, McCormick DA (2003) Barrages of synaptic activity control the gain and sensitivity of cortical neurons. *J Neurosci* 23(32):10388–10401.
4. Hô N, Destexhe A (2000) Synaptic background activity enhances the responsiveness of neocortical pyramidal neurons. *J Neurophysiol* 84(3):1488–1496.
5. Mitchell SJ, Silver RA (2003) Shunting inhibition modulates neuronal gain during synaptic excitation. *Neuron* 38(3):433–445.
6. Fernandez FR, Broicher T, Truong A, White JA (2011) Membrane voltage fluctuations reduce spike frequency adaptation and preserve output gain in CA1 pyramidal neurons in a high-conductance state. *J Neurosci* 31(10):3880–3893.
7. Higgs MH, Slee SJ, Spain WJ (2006) Diversity of gain modulation by noise in neocortical neurons: Regulation by the slow afterhyperpolarization conductance. *J Neurosci* 26(34):8787–8799.
8. Wolfart J, Debay D, Le Masson G, Destexhe A, Bal T (2005) Synaptic background activity controls spike transfer from thalamus to cortex. *Nat Neurosci* 8(12):1760–1767.
9. Deleuze C, et al. (2012) T-type calcium channels consolidate tonic action potential output of thalamic neurons to neocortex. *J Neurosci* 32(35):12228–12236.
10. Olsen SR, Bortone DS, Adesnik H, Scanziani M (2012) Gain control by layer six in cortical circuits of vision. *Nature* 483(7387):47–52.
11. Andolina IM, Jones HE, Wang W, Sillito AM (2007) Corticothalamic feedback enhances stimulus response precision in the visual system. *Proc Natl Acad Sci USA* 104(5):1685–1690.
12. Sillito AM, Jones HE (2002) Corticothalamic interactions in the transfer of visual information. *Philos Trans R Soc Lond B Biol Sci* 357(1428):1739–1752.
13. Halassa MM, et al. (2011) Selective optical drive of thalamic reticular nucleus generates thalamic bursts and cortical spindles. *Nat Neurosci* 14(9):1118–1120.
14. Swadlow HA, Gusev AG (2001) The impact of 'bursting' thalamic impulses at a neocortical synapse. *Nat Neurosci* 4(4):402–408.
15. Sherman SM (2001) Tonic and burst firing: Dual modes of thalamocortical relay. *Trends Neurosci* 24(2):122–126.
16. Lee S, Carvell GE, Simons DJ (2008) Motor modulation of afferent somatosensory circuits. *Nat Neurosci* 11(12):1430–1438.
17. Sirota MG, Swadlow HA, Beloozerova IN (2005) Three channels of corticothalamic communication during locomotion. *J Neurosci* 25(25):5915–5925.
18. Margrie TW, Brecht M, Sakmann B (2002) In vivo, low-resistance, whole-cell recordings from neurons in the anaesthetized and awake mammalian brain. *Pflugers Arch* 444(4): 491–498.
19. Groh A, Krieger P (2013) Structure-Function Analysis of Genetically Defined Neuronal Populations. *Cold Spring Harbor protocols* 2013(10).
20. Lu SM, Guido W, Sherman SM (1992) Effects of membrane voltage on receptive field properties of lateral geniculate neurons in the cat: Contributions of the low-threshold Ca2+ conductance. *J Neurophysiol* 68(6):2185–2198.

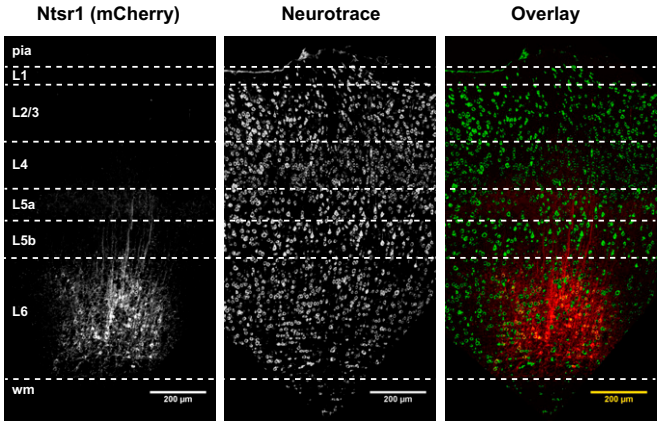

Fig. S1. Expression of ChR2-mCherry in BC deep layers. (*Left*) Virus-mediated expression of ChR2-mCherry in neurorensin receptor 1 (Ntsr1) neurons in the BC. Confocal scanning parameters were optimized to identify the expression of somata (low gain) and thereby confirm L6 specificity. mCherry expression in neuronal somata is restricted to L6 (see Fig. S2 for mCherry expression in the neuropil). (*Center*) Cortical layers were estimated by soma visualization using Neurotrace in the area shown in the left panel. (*Right*) Overlay of the left and middle panels. Somata are shown in green, and neurons expressing ChR2-mCherry are shown in red.

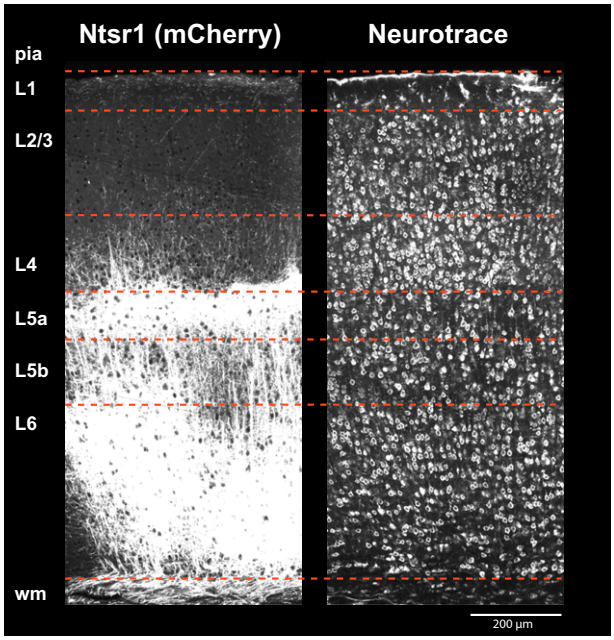

Fig. S2. Expression of ChR2-mCherry in BC. Confocal-scanning parameters were optimized to visualize dendritic expression (high gain). (*Left*) mCherry expression was strong in L6–L4 and dropped steeply in supragranular layers. (*Right*) Cortical layers shown in the left panel were estimated by soma visualization using Neurotrace. A noticeable portion of the fluorescence formed a band in L5a, and this signal may correspond to L6 intracortical axons as described for a subclass of cortico–thalamic L6 neurons (1). Very little signal was observed in L1, suggesting that, in contrast to visual cortex, Ntsr1 neurons do not have dendrites reaching L1 (2, 3).

1. Zhang ZW, Deschenes M (1997) Intracortical axonal projections of lamina VI cells of the primary somatosensory cortex in the rat: A single-cell labeling study. *J Neurosci* 17(16):6365–6379.
2. Lee CC, Lam YW, Sherman SM (2012) Intracortical convergence of layer 6 neurons. *Neuroreport* 23(12):736–740.
3. Olsen SR, Bortone DS, Adesnik H, Scanziani M (2012) Gain control by layer six in cortical circuits of vision. *Nature* 483(7387):47–52.

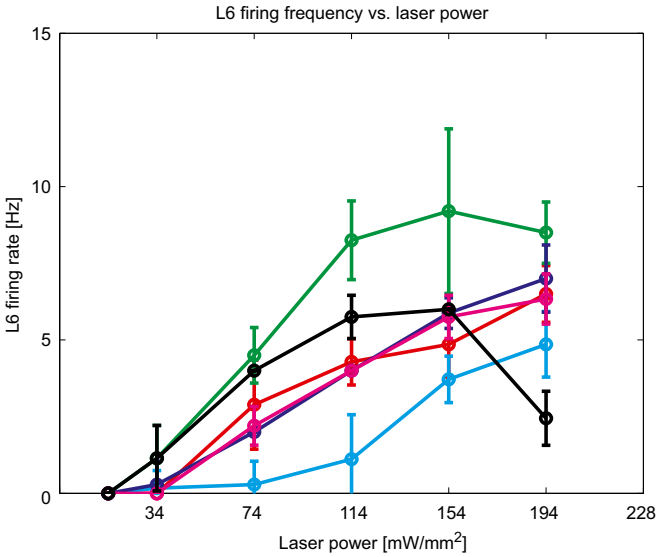

Fig. S3. Optogenetic activation profiles of Ntsr1 neurons. Activation of L6 neurons by laser pulses applied at different intensities (abscissa). Average spike firing frequencies (ordinate) were determined during a standard 500-ms laser pulse paradigm. Error bars indicate SD of laser responses of 15 pulse repetitions. Colors indicate different neurons ($n = 6$). Activation of Ntsr1 neurons with 74 mW/mm^2 for 500 ms evoked spike firing frequencies of ~4 Hz and was used as the standard paradigm.

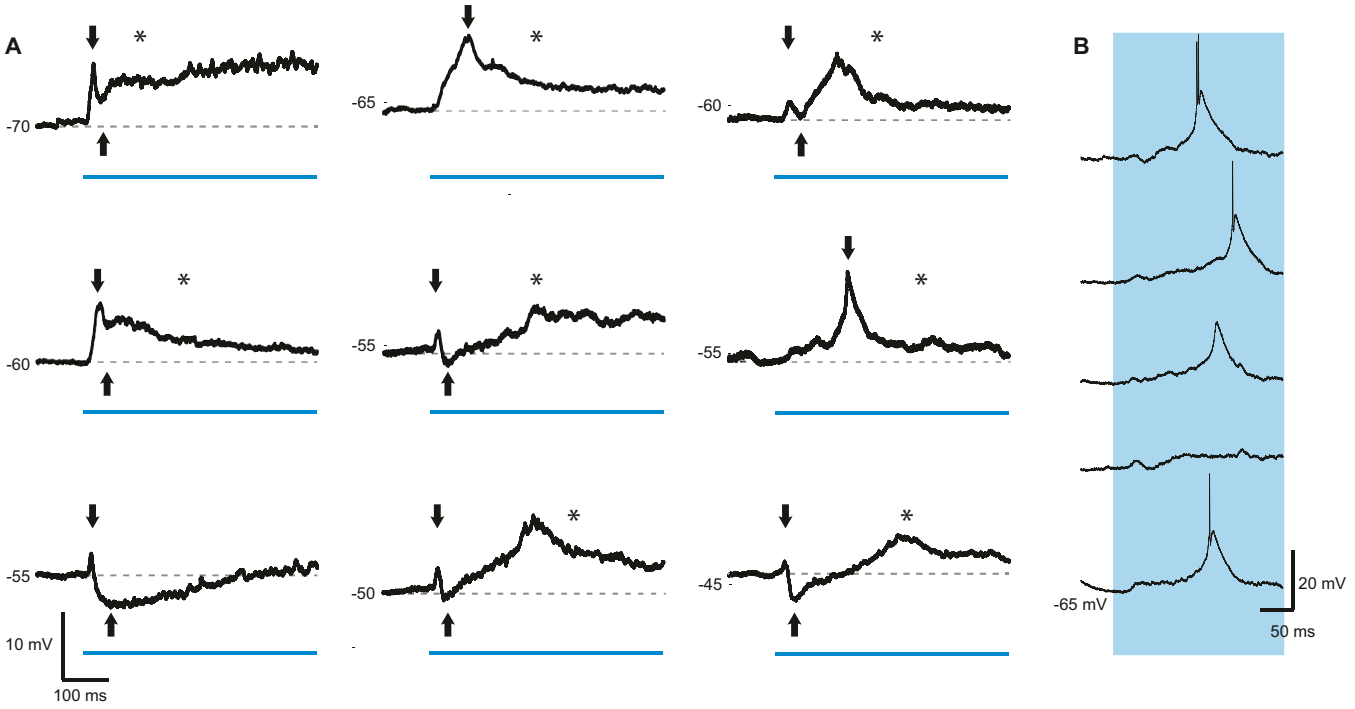

Fig. S4. VPM intracellular responses to Ntsr1 stimulation. (*A*) Average VPM intracellular responses to standard stimulation (74 mW/mm^2 for 500 ms)of Ntsr1 neurons (blue bar). Recordings are shown in ascending order of average resting membrane potential (RMP) (dashed line) as determined before the onset of stimulation. Downward/upward arrows indicate fast EPSP/IPSP, respectively and asterisks indicate steady state depolarization. The blue line indicates L6 stimulus. (*B*) Single trials from a recording in which L6 activation (blue) evoked delayed APs via slow activation of LTS (traces 1, 2, and 5), subthreshold LTS (trace 3), or failure (trace 4).

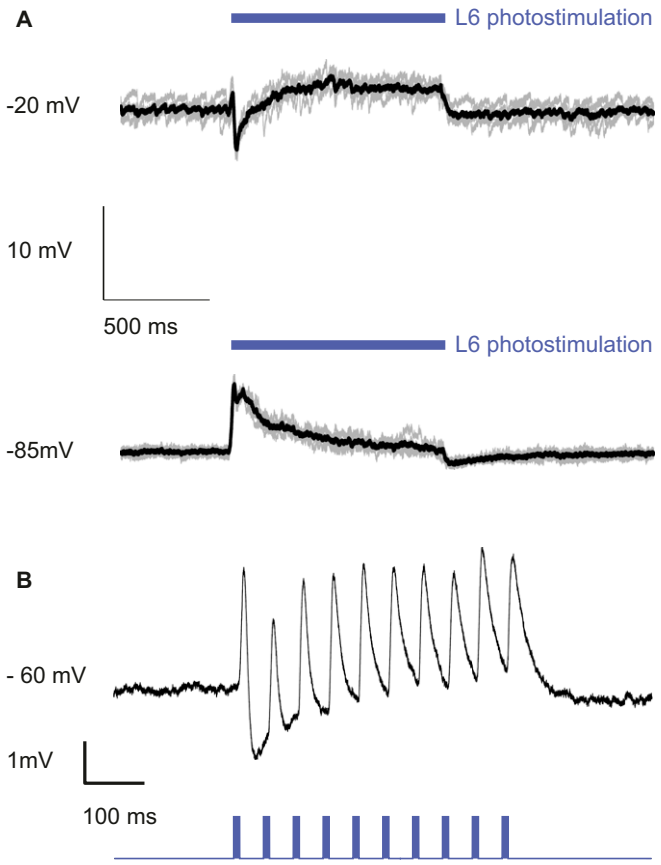

Fig. S5. L6-evoked depressing inhibitory postsynaptic potential (IPSP) in the VPM. (*A*) Median intracellular responses to L6 photostimulation (blue bar) in a VPM neuron at two different RMPs [−20 mV (*Upper*) and −85 mV (*Lower*)] reveals transient inhibitory input triggered by L6 activation. The gray traces show four superimposed repetitions. The black trace shows the median. Thus, in VPM neurons not showing hyperpolarization at normal RMPs, hyperpolarization could be detected when the membrane potential was depolarized by injecting current through the patch pipette, indicating a shunting effect through thalamic reticular nucleus recruitment. (*B*) L6 stimulation with stimulus trains (10-ms pulse length at 20 Hz) (blue). Average intracellular responses of eight repetitions show decreasing IPSPs.

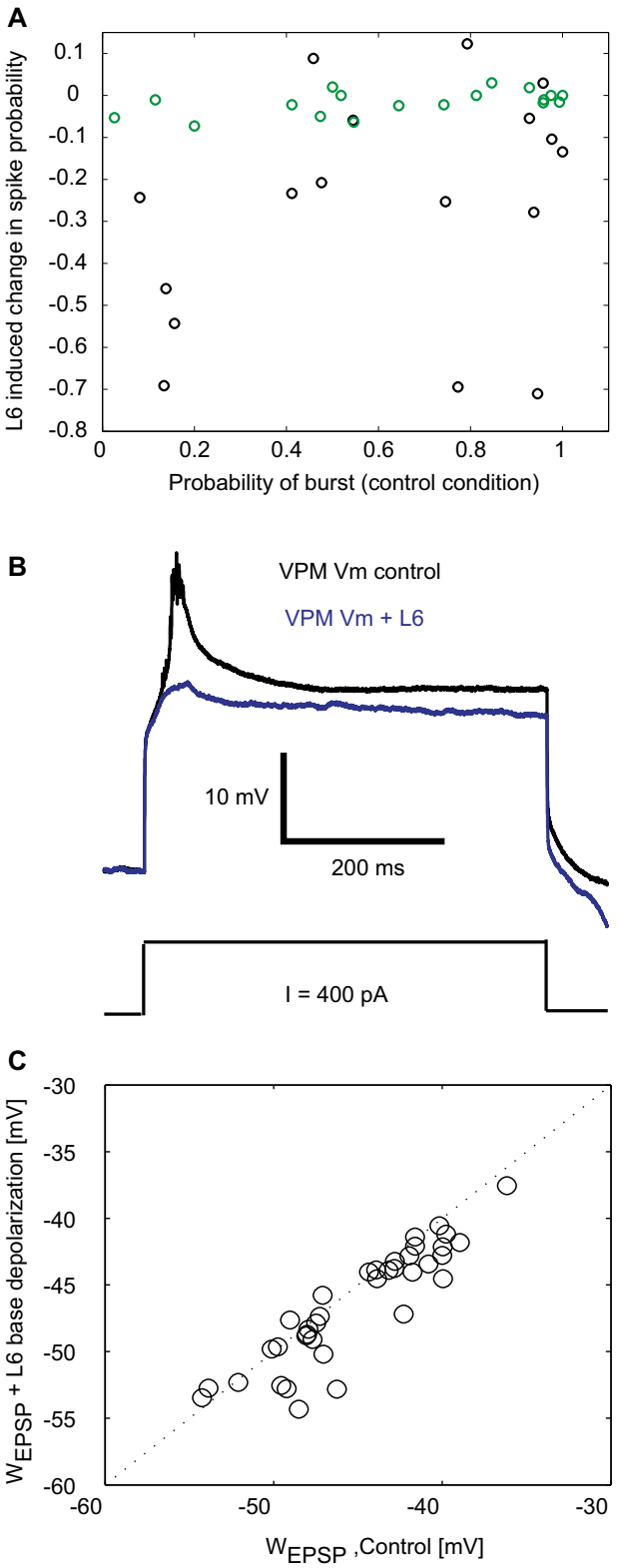

Fig. S6. Effect of L6 activation on spike probability, input resistance, and absolute EPSP peak. (*A*) Data showing the probability of a juxtacellular whisker response from 38 recordings and its dependence on L6 activity and control burstiness. Neurons in which the probability of response was changed significantly during L6 activation are indicated by black circles. Neurons that were unaffected are indicated by green circles. The probability of a spike after a single whisker stimulation was reduced significantly in approximately half of the neurons (17/38), was increased in 3/38 neurons, and was unchanged in the remainder of the recordings (18/38). The effect of L6 activity on the probability of a sensory-evoked spike is plotted over the probability of a burst in the control condition. There was no correlation between the L6-induced reduction in the probability of a spike response and the initial burstiness. (*B*) Measurement of input resistance of a VPM neuron in the control condition and with L6 stimulation. Current pulses were 500 ms long at a magnitude of 400 pA. Pulses without L6 stimulation were

Legend continued on following page

alternated with pulses of the same magnitude and duration in combination with L6 stimulation and were repeated 10 times. L6 stimulation reduced the input resistance determined from the average voltage at the end of the current injection (i.e., the average voltage at 450–500 ms). Average input resistances were 54.5 ±2 MΩ in the control condition and 39.3 ± 2.4 MΩ with L6 stimulation (n = 3). This result suggests that L6 activation increases the conductance of VPM neurons and thereby affects the probability of response. Note that APs were triggered in the control condition but not with L6 stimulation, as is consistent with an L6-induced reduction in the probability of response. (*C*) Whisker response peak (RMP + whisker EPSP magnitude) on a cell-by-cell basis with L6 stimulation vs. the control condition (using the cells and protocols shown in Fig. 3 *F–H*). Whisker response peak + L6 includes L6-induced depolarization. These data show that for isolated responses L6 depolarization did not always entirely compensate for the decrease in EPSP magnitude caused by that depolarization, possibly explaining the decrease in the probability of response shown in *A*.

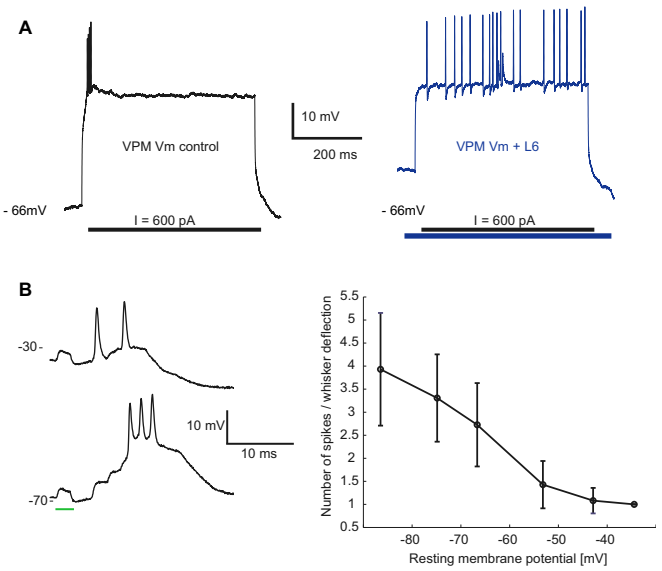

Fig. S7. (*A*) L6 activation promotes tonic responses when APs are elicited by current injections. Tonic switch is independent of sensory input. (*Left*) Injections of current (500 ms, 400–600 pA) elicited typical burst APs in control conditions. (*Right*) When the same current injection was combined with L6 stimulation, a train of tonic APs was elicited. Similar results were observed in three independent experiments. (*B*, *Left*) Tonic whisker responses can also be promoted by depolarization via the injection of current. As observed with L6 stimulation, depolarization by the injection of current switched the response mode in a graded manner. Intracellular whisker responses were measured at different membrane potentials controlled by injection of current. The upper voltage trace shows an example of a response during depolarization with the injection of current, and the lower voltage trace shows a response at the control membrane potential. (*Right*) The graph summarizes how burstiness, as measured as the number of spikes per response, decreases with depolarization. Only successful whisker responses were considered. Similar results were observed in three independent experiments. To confirm that the RMP underlies this switch in firing mode, we elicited APs independent of sensory stimulation via stepped injections of current (600 pA, 500 ms), triggering a typical short burst response comparable to that observed with whisker stimulation. As in the sensory stimulation paradigm, L6 stimulation changed the response to the same injection of current into a typical tonic AP train as a result of the depolarizing L6 input inactivating the I_T conductance (Fig. S6).

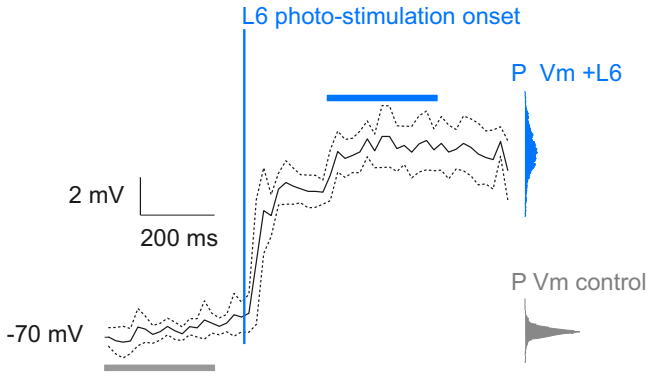

Fig. S8. L6-induced increase in VPM membrane potential fluctuations. Mean VPM membrane potential (σ) (black solid line) ± SD (dotted lines) in a recording before and after L6 activation. The vertical blue line shows the onset of L6 activation. The membrane potential σ for the two conditions was calculated from windows extracted 300 ms before the onset of L6 activation (gray bar; control condition) and 200 ms after L6 activation (blue bar). Histograms to right show membrane potential distributions (gray, without L6, σ = 0.8 mV; blue, with L6 activation, σ =1.1 mV). For the nine neurons tested with this protocol, the resulting membrane potential σ ranged from 0.15–0.8 mV in the control condition and from 0.8–1.1 mV with L6 activation. Eight of the nine VPM neurons showed a significant increase in membrane potential σ (two-sample F-test, $P < 0.01$), with a median increase of 83%, first quartile 46%, third quartile 126% (paired Wilcoxon signed rank test, $P < 0.01$).